Wiley
International Transactions on Electrical Energy Systems
Volume 2024, Article ID 7392391, 9 pages
https://doi.org/10.1155/2024/7392391

Research Article

Effect of Sensor Faults on the Stresses Caused by Wind Turbine Blades

Dariush Biazar

Department of Electrical and Computer Engineering, Ramsar Branch, Islamic Azad University, Ramsar 4691966434, Iran

Correspondence should be addressed to Dariush Biazar; dbiazar@yahoo.com

Received 12 December 2023; Revised 30 January 2024; Accepted 22 February 2024; Published 23 May 2024

Academic Editor: Sujin Bureerat

Rotor blades are the main part for generating electrical energy and the primary source of stresses in a wind turbine (WT). The stresses caused by the blades increase the load on the hub, tower, and foundation of the WTs. In this research, the asymmetry of the blade angle with each other has been investigated as one of the factors affecting the stress distribution using Monte Carlo (MC) simulation. The focus of this study is on the stresses caused by the asymmetry of the blades angle when there is the fault in the sensors. A deep understanding of the blade stress distribution due to sensor faults can improve control designs, increase WT operating time, and reduce energy generation costs when these faults occur.

1. Introduction

Wind energy has experienced rapid and significant development in recent decades. It is now the main source of renewable energy and has provided about 6% of total world electricity demand in 2018 [1]. As WTs grow, designers and investors pay more attention to improving efficiency and reducing costs to make them more competitive. However, O&M of wind power systems accounts for 25–30% of the total energy production cost [2]. Therefore, reducing the cost of repairs in WTs makes the production of this energy more competitive [3–7]. Maintenance costs largely depend on the number, type, and severity of faults; therefore, early prediction of faults can reduce their severity or even prevent them from occurring.

The disadvantages of blades have always been of interest to investors due to their high O&M costs [8–11]. The deviation of PABs with each other and the deviation between the reference and real PABs are one of the important defects of WT blades, which causes the asymmetry of the blades and causes stress and damage to the gearbox and tower [12–15]. As the stress increases, the WT must be stopped to avoid damage to its components and structure.

Fault in the WT sensors is one of the main reasons for asymmetry in the blades. Dust, salt spray, lightning, corrosion, and humidity are some of the factors that can affect the performance of sensors. Also, sensors are easily damaged by repairmen. Therefore, understanding the effect of sensors fault on other WT parameters is very important for control system designers for better performance of controllers when these faults occur. In this case, one of the actions is that a new set of sensors that are in good condition can be configured to send the appropriate measurement signals to the control system [16]. Considering that more than 14% of the WT faults occur in sensors [17, 18], therefore the focus of this research is on stresses caused by asymmetry of the PABs when fault occurs in sensors.

The WT equations are complex and nonlinear, so the analytical method cannot be easily used to analyze the effects of fault in sensors on the PABs and output power. In this paper, the MC method is used to evaluate these faults, because it provides a more accurate description of the system performance, thus allowing further analysis. Today, this method is used in many engineering fields to evaluate the reliability of complex systems. MC methods provide a description of the output function according to a set of random numbers as input. In these methods, the inputs are selected as the probability density function that best matches the real conditions [19, 20].

In this research, we model fault in sensors with a Gaussian probability distribution function. Then, according to the MC simulation technique, a series of random samples are generated, and in each iteration, a sample of it is applied to the system for simulation as a fault.

2. The WT Model and Control Strategy

The control diagram of a WT system with a horizontal three-bladed axis is shown in Figure 1. It consists of four main subsystems: the blade pitch; drivetrain; generator; and converter and controller. The controller receives the measured values from sensors such as the PAB, generator speed, and output power and adjusts PABs ($\beta_{1,2,3\,\mathrm{ref}}$) and generator torque ($\tau_{g\,\mathrm{ref}}$). The nonlinear equation of the WT model is written as follows [21, 22]:

$$\begin{aligned}
\dot{x} &= f(x) + Bu,\\
x &= \left[\omega_r, \omega_g, \theta, \beta, \dot{\beta}, \tau_g\right]^T,\\
u &= \left[\beta_{\mathrm{ref}}, \tau_{\mathrm{ref}}\right]^T,\\
f(x) &= \begin{bmatrix} \dfrac{\tau_r(x_1, x_4)}{J_r} - \dfrac{(B_{dt} + B_r)}{J_r}x_1 + \dfrac{B_{dt}}{N_g J_r}x_2 - \dfrac{K_{dt}}{J_r}x_3 \\[2ex] \dfrac{\eta_{dt}\cdot B_{dt}}{N_g J_g}x_1 - \left(\dfrac{\eta_{dt}\cdot B_{dt}}{N_g^2 J_g} + \dfrac{B_g}{J_g}\right)x_2 + \dfrac{\eta_{dt}\cdot K_{dt}}{N_g J_g}x_3 - \dfrac{1}{J_g}x_6 \\[2ex] x_1 - \dfrac{1}{N_g}x_2 \\[2ex] x_5 \\[2ex] -\omega_n^2 x_4 - 2\zeta\omega_n x_5 \\[2ex] -\dfrac{1}{\alpha_g}x_6 \end{bmatrix},\\
B &= \begin{bmatrix} 0, 0, 0, 0, 0, \dfrac{1}{\alpha_g} \\[2ex] 0, 0, 0, 0, \omega_n^2, 0 \end{bmatrix}^T,
\end{aligned} \tag{1}$$

where x is the state vector, u is the control input, and $f(x)$ is the nonlinear vector. The main purpose of operating the WT is to maximize production capacity while minimizing operating costs, which depends on its operating regions. These regions are divided into four operational regions according to wind speed, as shown in Figure 2, which shows the output power, pitch angle, and power coefficient for optimal WT performance [23]. The WTs do not generate energy at wind speeds lower than $\mathrm{Cut}_{\_\mathrm{in}}$ (region I) due to increased operating costs versus generated power and at wind speeds higher than $\mathrm{Cut}_{\_\mathrm{out}}$ (region IV) to avoid stress increases and should be stopped. However, since electrical power is generated in both the PL (II) and FL (III) regions, the two main control strategies are used as shown in Figure 1. In region II, by adjusting the dual-mode switch in Figure 1 in position I, the control system keeps the blades closed and controls the generator torque to generate energy.

In region III, by adjusting the dual-mode switch in Figure 1 in position II, the control system changes the PABs to maximize output power while minimizing structural and mechanical stress on the rotor blades. For a detailed description of the principle of operation of the WT system, you can refer to [24, 25]. For this research, the WT model with an output power of 4.8 MW has been used in the simulation, which is directly taken from [26, 27].

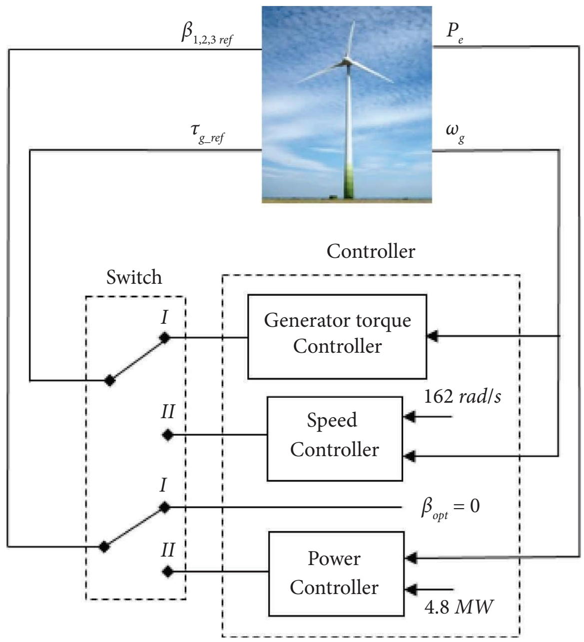

Figure 1: The WT and controllers.

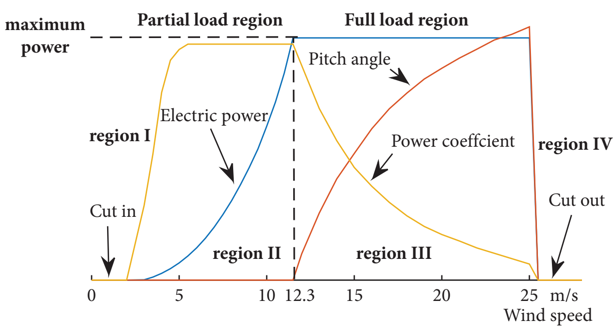

Figure 2: Operational regions of the WT.

3. Description of Sensor Faults

The types of faults that occur in sensors are the multiplicative fault, output stuck on a fixed value, bias fault, and slow drifting fault [16]:

(i) Bias fault $M_i^f = M_i + \Delta f_i$

(ii) Multiplicative fault $M_i^f = \delta M_i$, where $0 \leq \delta$

(iii) Output stuck $M_i^f = C_0$; C_0 is a constant

(iv) Slow drifting $M_i^f = M_i + \alpha t$, α is a small variation rate, and t is the time

where M_i is the actual output of the sensors and Δf_i and C_0 are the sensor faults, which are assumed to be a Gaussian probability distribution.

In this study, to investigate the effect of faults, we assume that only one fault occurs in the sensor at a time, and we do not consider the slow drifting fault in the sensor. To simulate the disconnection of the sensor, we assume a multiplicative fault with $\delta = 0$. It is clear that when the sensor is disconnected (if there is no redundant sensor), the turbine must stop. Our goal is to investigate the effect of sensor disconnection performance on the blade angle and WT performance. Table 1 shows the faults that occur in different sensors [26, 27]. Considering that the blade control mechanism in WT is not active in region II, therefore simulations are performed only in region III.

4. Analysis of the Effect of Fault in Sensors on Structural Stresses

Table 2 shows the output values of the sensors in normal operating conditions and with a wind speed of 22 m/s, as well as the values of parameters of the Gaussian fault probability function applied to the sensors. According to Table 1, we simulate the changes in output power and the PAB in WT with 200 random samples of different faults by the MC method. Considering that our focus is on investigating the impact of faults on wind turbine performance, we have chosen 200 samples randomly and hypothetically. Increasing or decreasing the number of samples under investigation does not affect the results. Considering that the output data of the sensors follow the Gaussian distribution function due to systematic errors, therefore, in this paper, this distribution is used to analyze the faults. To investigate the effect of each fault, a random sample is generated according to its Gaussian probability density function. Then, this sample as Δf_i or C_0 is applied to the simulation system as a fault in each iteration.

It should also be noted that in the full-load region, due to drastic changes in all variables of the WT, if the power sensor or the speed and torque sensors of the generator are disconnected, it is not possible to simulate. Therefore, the effects of these faults are similar to the output stuck in the relevant sensors. In the following, we will analyze the performance of the WT by applying the faults mentioned in Section 3 on the four sensors of the blade angle, speed, and torque of the generator and power sensor.

4.1. The PAB Sensor. To simulate faults in this sensor, we assume that the fault occurs only in the PAB1 sensor.

4.1.1. Bias in Sensor Output. Despite this fault, the controllers correct the tracking to keep the output power constant. But as shown in curve F11 in Figure 3, this fault causes a change in the angle in the other two blades. That is, with a positive bias fault in the PAB1 sensor, the controller reduces the angle of the other two blades to reach the nominal output power, and conversely, with a negative bias fault in this sensor, the angles of the other two blades open more. Due to the asymmetry in the PABs with each other, stresses on the WT increase.

4.1.2. Sensor Output Stuck. By applying this fault to the sensor, a constant value is applied to the speed controller. In this case, the controller sends the wrong signal to the blades actuator. According to the F12 curve in Figure 3, it is clear that this fault has a large effect on the output power, so that

Table 1: Sensor faults in the WT.

No. fault	Sensor faults
F11	Pitch sensor (1, 2, 3), output bias
F12	Pitch sensor (1, 2, 3), output stuck
F13	Pitch sensor (1, 2, 3), cut off
F21	Generator speed sensor, output bias
F22	Generator speed sensor, output stuck
F23	Generator speed sensor, cut off
F31	Generator torque sensor, output bias
F32	Generator torque sensor, output stuck
F33	Generator torque sensor, cut off
F41	Power sensor, output bias
F42	Power sensor, output stuck
F43	Power sensor, no output

Table 2: Nominal sensor values and fault parameters.

No. fault	Nominal value of sensor output	Gaussian fault parameters	
		Average	Standard deviation
F11		0°	5°
F12	20.5°	21°	5°
F13		—	—
F21		0 rad/s	5 rad/s
F22	162 rad/s	162 rad/s	5 rad/s
F23		0 rad/s	10 rad/s
F31		0 N/m	5000 N/m
F32	29630 N/m	29000 N/m	2000 N/m
F33		—	—
F41		0 W	100 kW
F42	4.8*e*6 W	4.8*e*6 W	500 kW
F43		—	—

the controllers are not able to fully compensate for this fault, and the higher the value of this fault, the greater the output power error. If the constant output value of the PAB 1 sensor is less than the angle value of the other two blades, the controllers try to control the WT power by increasing the angle of blades 2 and 3. However, if the constant output of the PAB 1 sensor is greater than the value of the other two blade angles, the output power decreases and the controller reduces the angle of blades 2 and 3 to control power. In this case, the structural loads increase significantly, which can cause severe damage to the WT and environs.

4.1.3. Sensor Cutoff. According to the F13 curve in Figure 3, with this fault, one of the blades cannot control the output power. In this case, the sensitivity of the output power to the PABs 2 and 3 is maximized and the controllers open the angle of blades 2 and 3 more to control the output power. In this situation, the stresses in the WT increase and should be stopped.

4.2. Generator Speed Sensor

4.2.1. Bias in Sensor Output. The output power remains almost constant with different bias faults in this sensor. According to curve F21 in Figure 4, the angle of all blades decreases with a positive bias fault in the generator sensor. Conversely, with a negative bias fault in the sensor, the angle of all blades increases.

4.2.2. Output Stuck or Sensor Cutoff. According to the F22 curve in Figure 4, a stuck output or an interrupted fault in this sensor will cause the blades to not rotate properly. Depending on the fixed value in the sensor output, all the blades open or close. In this situation, the output power cannot be controlled due to drastic changes in variables and increases stress, which will be very dangerous for the safety of the WT.

4.3. Generator Torque Sensor

4.3.1. Bias in Sensor Output. As can be seen from the simulation results of the F31 curve in Figure 5, this fault will have a small effect on the production power, because the controllers compensate for the power and speed tracking. However, a positive bias fault in this sensor opens the blades for more power output control, and conversely, a negative bias fault in this sensor causes the turbine blades to close more.

4.3.2. Output Stuck or Sensor Cutoff. The output stuck fault of this sensor is checked in two cases. The first case, as shown in curve F32 in Figure 5, is when the fixed value output of this sensor is less than its nominal value in Table 2, which reduces the angle of the blades and eventually closes. But in the second case, if the fixed value output of this sensor is more than the nominal value, the generated power will increase and the angle of the blades is fully opened (in this case, the power fluctuates for values close to the nominal value).

The disconnection of this sensor in region III causes the sudden closing of the WT blades. These conditions cause the torques applied to the generator and rotor to increase suddenly, resulting in increased stress, and the WT must be shut down immediately.

4.4. Power Sensor

4.4.1. Bias in Sensor Output. The bias fault in this sensor will have little effect on the output power, so that the controllers compensate for power and speed tracking. According to the F41 curve in Figure 6, positive bias fault in this sensor causes the blades to open slightly to control the output power, and conversely, a negative bias fault causes the blades of the WT to close more. The changes in the angle of blades will be small with this fault.

4.4.2. Output Stuck or Sensor Cutoff. According to the F42 curve in Figure 6, the output stuck fault in this sensor is checked in two cases. The first case is when the fixed output of this sensor is less than the nominal value. In this case, the blade angle is reduced and finally closed in a short period. The closing time of the PABs depends on the fixed value

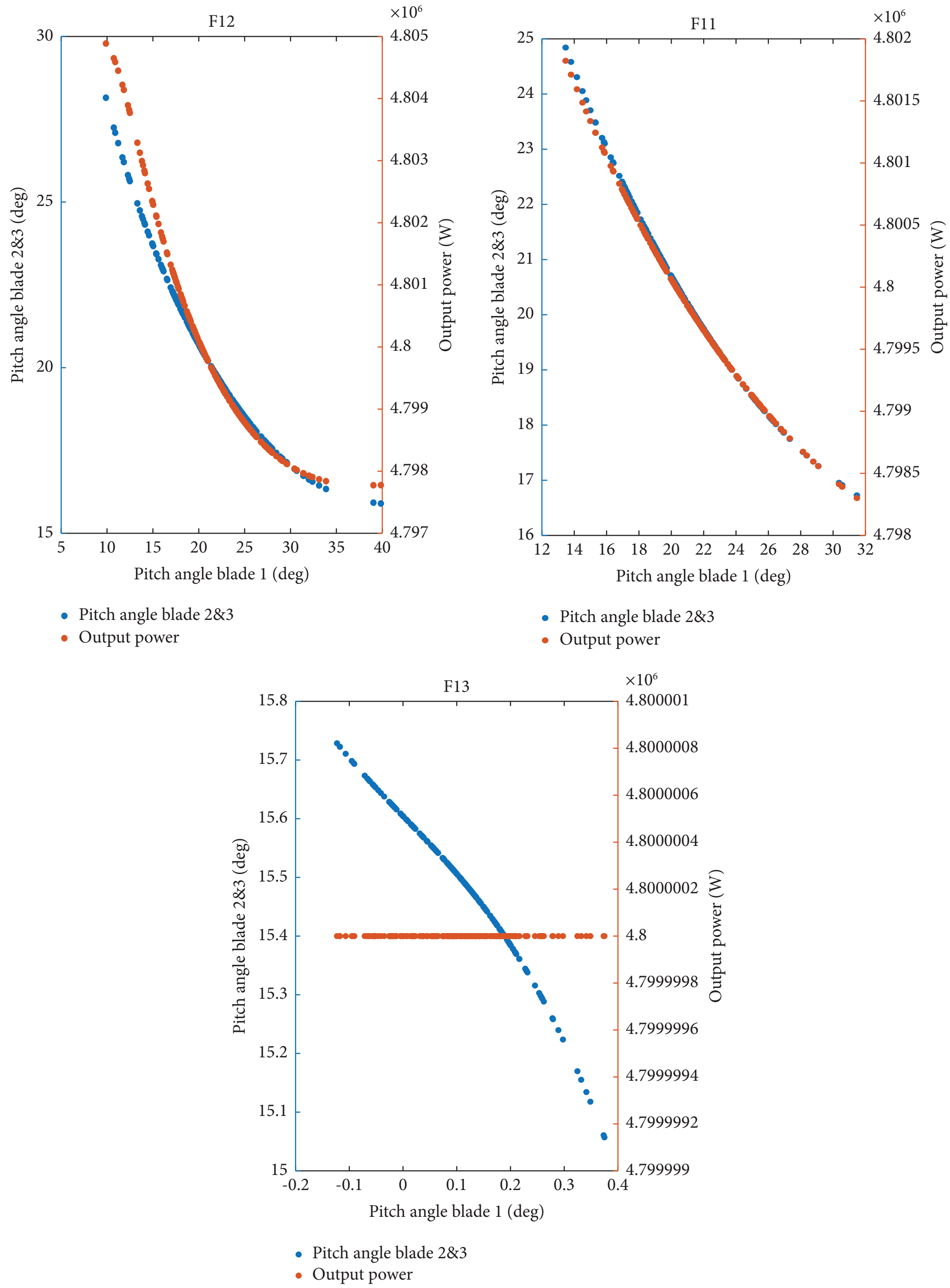

Figure 3: Effect of faults on the PAB1 sensor.

output of the power sensor. The closer the fixed value of the power sensor is to the normal value, the longer it takes for the blades to close. But in the second case, if the fixed value of this sensor is greater than the nominal value, the angle of blades in this case opens completely. In both cases, the output power changes will be high.

The disconnection of this sensor, like the generator torque sensor, causes the sudden closing of the WT blades.

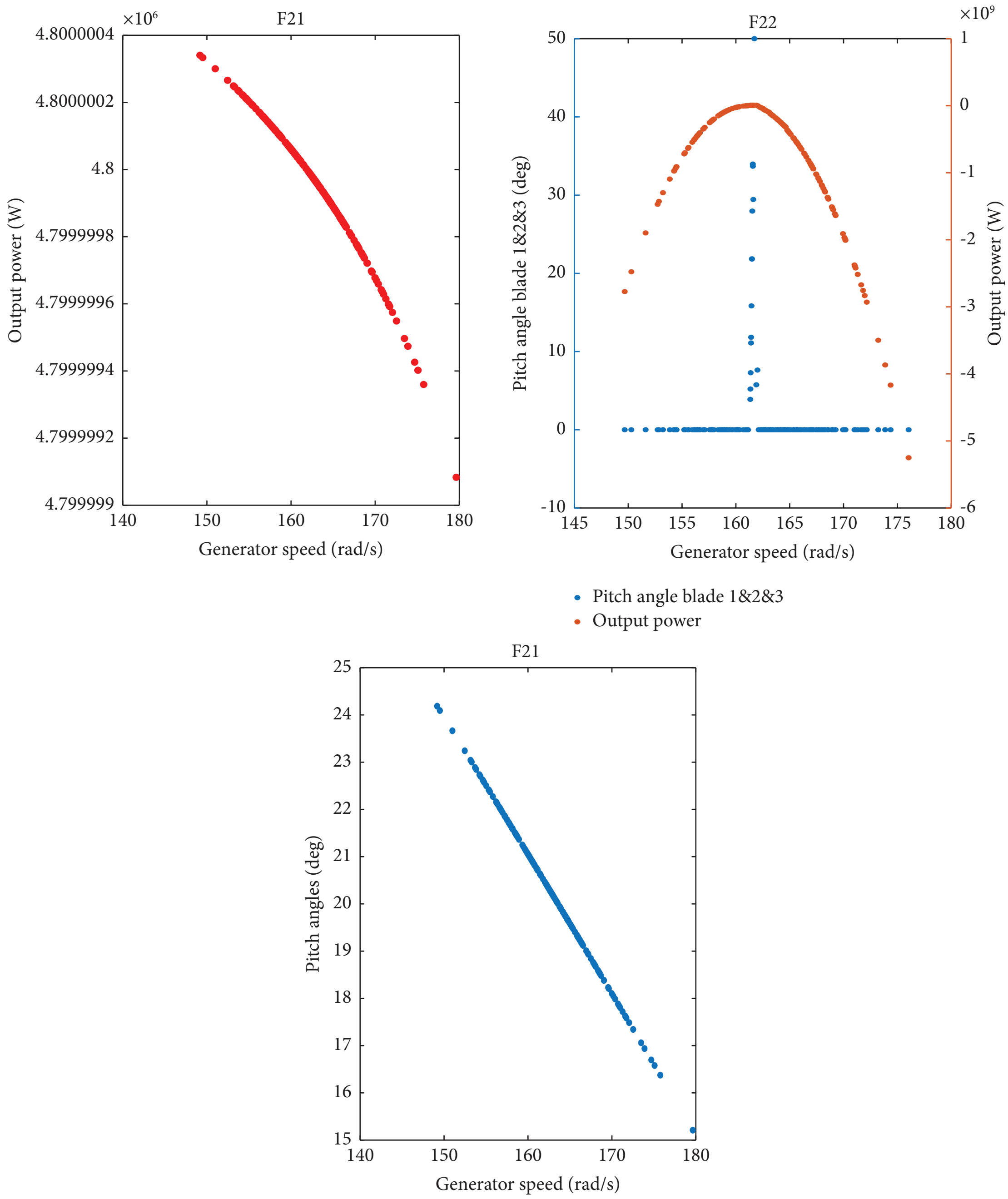

Figure 4: Effect of faults on the generator speed sensor.

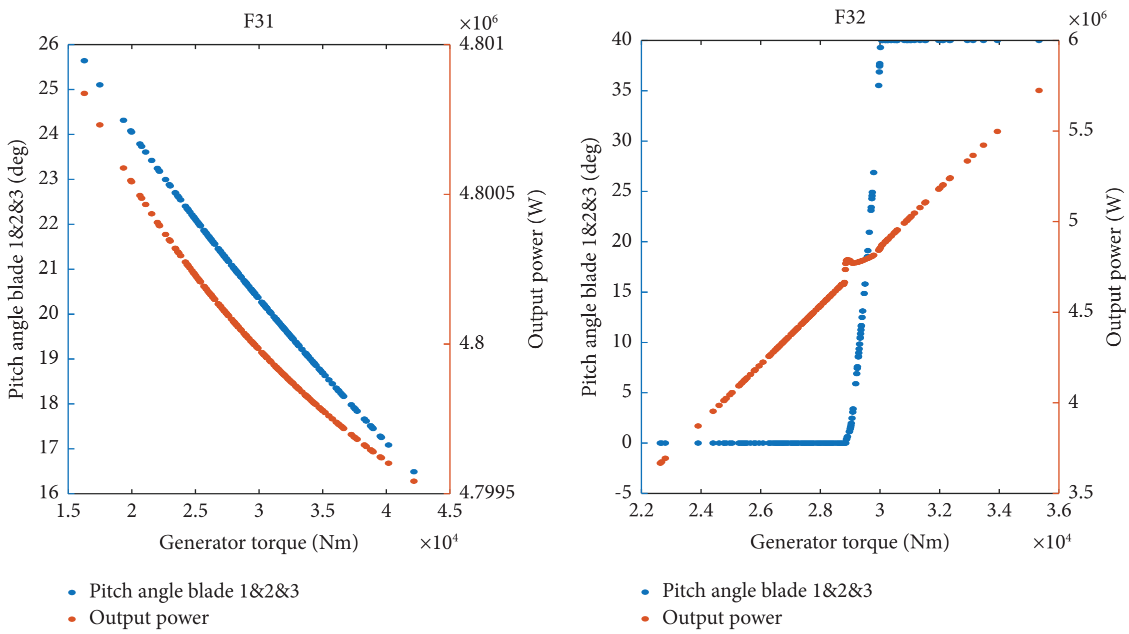

Figure 5: Effect of faults on the generator torque sensor.

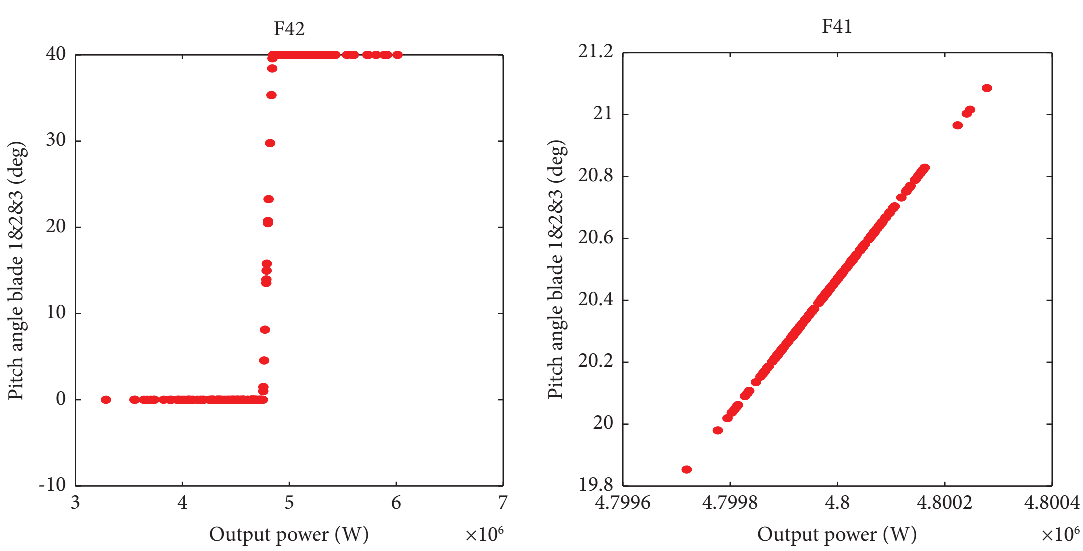

Figure 6: Effect of faults on the power sensor.

Table 3: Results of faults in sensors.

No. fault	Description of the stress	Action
F11	With the bias fault in the PAB 1 sensor, the angle of the other two blades changes. With increasing bias, the asymmetry between the PABs increases, so the stress increases and the WT must be shut down	Shut down
F12	The control system changes the angle of the other two blades with this fault, which results in the PAB asymmetry and increases the stress, and the WT must be shut down	Shut down
F13	The control system further opens PABs 2 and 3. In this case, the stresses in the tower increase and the WT must be shut down	Shut down
F21, F31, F41	With these faults, the control system changes the angle of all blades equally. Therefore, there is no stress due to asymmetry of the blades	—
F22, F23, F32, F33, F42, F43	In this case, the PABs maximize or minimize suddenly. This condition will be very dangerous for WT safety due to increased stress, and the WT must be shut down	Shut down

In this condition, the torques applied to the generator and rotor suddenly increase, resulting in an increase in stress, and the WT must be shut down immediately.

5. Conclusion

In this research, we investigated the stresses caused by the asymmetry of the blades in the WT caused by the faults in the four main sensors of the control system. For each sensor, we considered three faults as the Gaussian probability distribution. Then, using the MC method, we simulated and analyzed their effect on PABs and the power produced in WT. Table 3 summarizes the simulation results. Using the results of the analysis, it is determined that except for the bias fault in the speed and torque sensors of the generator and the power sensor, the occurrence of other faults in the sensors will require WT to be shut down. The designer of the control system should consider these sensors as redundant to increase the reliability of WT. In this case, it leads to increased profitability and more efficient performance of WTs.

Nomenclature

Variables

$\beta_{1,2,3}$: Pitch angle of the blade WT (wind turbine)
τ_r: Rotor torque MC (Monte Carlo)
τ_g: Generator torque FLR (full-load region)
ω_g: Generator speed PLR (partial-load region)
ω_r: Rotor speed O&M (operation and maintenance)
P_{out}: Power in the WT PAB (pitch angle of blade)
R: Radius of the blades
v_w: Wind speed
J_r: Moment of inertia of the low-speed shaft
K_{dt}: Torsion stiffness of the drivetrain
B_{dt}: Torsion damping coefficient of the drivetrain
B_g: Viscous friction of the high-speed shaft
B_r: Viscous friction of the low-speed shaft
N_g: Gear ratio
J_g: Moment of inertia of the high-speed shaft
η_{dt}: Efficiency of the drivetrain
α_g: Generator and converter model parameter

Abbreviations

WT: Wind turbine
FLR: Full-load region
PLR: Partial-load region
O&M: Operation and maintenance
PAB: Pitch angle of blade.

Data Availability

The data used to support the findings of this study are included within the article.

Conflicts of Interest

The author declares that there are no conflicts of interest.

References

[1] World Wind Energy Association Wwea, *Wind Power Capacity Worldwide Reaches 597 GW, 50.1 GW Added in 2018*, WWEA, Bonn, Germany, 2019.

[2] F. Ding, Z. Tian, and T. Jin, "Maintenance modeling and optimization for wind turbine systems: a review," in *Proceedings of the 2013 International Conference on Quality, Reliability, Risk, Maintenance, and Safety Engineering (QR2MSE)*, Chengdu, China, July 2013.

[3] D. B. Nelson, M. H. Nehrir, and C. Wang, "Unit sizing and cost analysis of stand-alone hybrid wind/PV/fuel cell power generation systems," *Renewable Energy*, vol. 31, no. 10, pp. 1641–1656, 2006.

[4] C. A. Walford, "Wind turbine reliability: understanding and minimizing wind turbine operation and maintenance costs," SANDIA Report, pp. 1–26, Sandia National Laboratory, Livermore, CA, USA, 2006.

[5] G. Joselin Herbert, S. Iniyan, E. Sreevalsan, and S. Rajapandian, "A review of wind energy technologies," *Renewable and Sustainable Energy Reviews*, vol. 11, no. 6, pp. 1117–1145, 2007.

[6] J. Tautz-Weinert and S. J. Watson, "Using SCADA data for wind turbine condition monitoring- a review," *IET Renewable Power Generation*, vol. 11, no. 4, pp. 382–394, 2017.

[7] W. Yang, Z. Peng, K. Wei, and W. Tian, "Structural health monitoring of composite wind turbine blades: challenges, issues and potential solutions," *IET Renewable Power Generation*, vol. 11, no. 4, pp. 411–416, 2017.

[8] Z. Zhang, B. Fan, Y. Liu, P. Zhang, J. Wang, and W. Du, "Rapid warning of wind turbine blade icing based on MIV-tSNE-RNN," *Journal of Mechanical Science and Technology*, vol. 35, no. 12, pp. 5453–5459, 2021.

[9] Z. Liu, X. Wang, and L. Zhang, "Fault diagnosis of industrial wind turbine blade bearing using acoustic emission analysis," *IEEE Transactions on Instrumentation and Measurement*, vol. 69, no. 9, pp. 6630–6639, 2020.

[10] R. W. Hyers, J. G. McGowan, K. L. Sullivan, J. F. Manwell, and B. C. Syrett, "Condition monitoring and prognosis of utility scale wind turbines," *Energy Materials*, vol. 1, no. 3, pp. 187–203, 2006.

[11] H. Garg and R. Dahiya, "Current signature analysis and its application in the condition monitoring of wind turbine for rotor faults," *Energy Syst*, vol. 8, no. 3, pp. 495–510, 2017.

[12] M. L. Wymore, J. E. Van Dam, H. Ceylan, and D. Qiao, "A survey of health monitoring systems for wind turbines," *Renewable and Sustainable Energy Reviews*, vol. 52, no. 2, pp. 976–990, 2015.

[13] E. Hart, B. Clarke, G. Nicholas et al., "A review of wind turbine main-bearings: design, operation, modelling, damage mechanisms and fault detection," *Wind Energy Science*, vol. 5, no. 1, pp. 105–124, 2020.

[14] K. Fischer, F. Besnard, and L. Bertling, "Reliability-centered maintenance for wind turbines based on statistical analysis and practical experience," *IEEE Transactions on Energy Conversion*, vol. 27, no. 1, pp. 184–195, 2012.

[15] H. J. Sutherland and J. F. Mandell, "Effect of mean stress on the damage of wind turbine blades," *Journal of Solar Energy Engineering*, vol. 126, no. 4, pp. 1041–1049, 2004.

[16] X. Wei, M. Verhaegen, and T. van den Engelen, "Sensor Fault diagnosis of wind turbines for fault tolerant," *IFAC Proceedings Volumes*, vol. 41, no. 2, pp. 3222–3227, 2008.

[17] J. Ribrant and L. M. Bertling, "Survey of failures in wind power systems with focus on Swedish wind power plants

during 1997–2005," *IEEE Transactions on Energy Conversion*, vol. 22, no. 1, pp. 167–173, 2007.

[18] L. Zhou, Q. Zhao, X. Wang, and A. Zhu, "Fault diagnosis and reconstruction of wind turbine anemometer based on RWSSA-AANN," *Energies*, vol. 14, no. 21, p. 6905, 2021.

[19] R. Billinton and P. Wang, "Teaching distribution system reliability evaluation using Monte Carlo simulation," *IEEE Transactions on Power Systems*, vol. 14, no. 2, pp. 397–403, 1999.

[20] A. Crespo Marquez, A. Sánchez Heguedas, and B. Iung, "Monte Carlo-based assessment of system availability: a case study for cogeneration plants," *Reliability Engineering & System Safety*, vol. 88, no. 3, pp. 273–289, 2005.

[21] S. Dey, P. Pisu, and B. Ayalew, "A comparative study of three fault diagnosis schemes for wind turbines," *IEEE Transactions on Control Systems Technology*, vol. 23, no. 5, pp. 1853–1868, 2015.

[22] D. Biazar, H. Khaloozadeh, and M. Siahi, "Sensitivity analysis for evaluation of the effect of sensors error on the wind turbine variables using Monte Carlo simulation," *IET Renewable Power Generation*, vol. 16, no. 8, pp. 1623–1635, 2022.

[23] K. E. Johnson, L. Y. Pao, M. J. Balas, and L. J. Fingersh, "Control of variable-speed wind turbines: standard and adaptive techniques for maximizing energy capture," *IEEE Control Systems Magazine*, vol. 26, no. 3, pp. 70–81, 2006.

[24] Y. M. Saint-Drenan, R. Besseau, M. Jansen et al., "A parametric model for wind turbine power curves incorporating environmental conditions," *Renewable Energy*, vol. 157, pp. 754–768, 2020.

[25] P. F. Odgaard, J. Stoustrup, and M. Kinnaert, "Fault-tolerant control of wind turbines: a benchmark model," *IEEE Transactions on Control Systems Technology*, vol. 21, no. 4, pp. 1168–1182, 2013.

[26] T. Esbensen and C. Sloth, "Fault diagnosis and fault-tolerant control of wind turbines," Master Thesis, University of Aalborg, Denmark, Europe, 2009.

[27] D. Biazar, H. Khaloozadeh, and M. Siahi, "Evaluating the effect of wind turbine faults on power using the Monte Carlo method," *Wind Energy*, vol. 25, no. 5, pp. 935–951, 2022.